Development Program for the F-15 Inlet

William F. Imfeld*
Aeronautical Systems Division, Wright-Patterson Air Force Base, Ohio

This paper describes the F-15 variable capture area inlet and the associated control system. Factors that influenced integration of the inlet/inlet control system with the total airframe are discussed. The methodology of using instantaneous total pressure patterns at the engine face to evaluate the effect of inlet distortion on engine operation is briefly described. Several inlet design variables that were tested are discussed. In addition to its effects on inlet behavior, the variable capture area reduces cruise drag, favorably influences aircraft longitudinal stability at low speeds, and reduces loads on the inlet backup structure at certain supersonic conditions. The boundary-layer bleed system optimization demonstrated that a slot in the throat was the single most effective location for bleed removal. Comparative results are presented for the final configuration between model and full-scale wind-tunnel testing, and subsequent flight testing. Results show that full-scale instantaneous distortion typically is equal to or less than that measured on a 1/6th scale model.

Nomenclature

A_0/A_c	= mass flow ratio
C_L	= lift coefficient
C_m	= pitching moment coefficient
K_{A_2}	= fan distortion index
M_0	= freestream Mach number
M_{th}	= inlet throat Mach number
P_0	= freestream static pressure
P_{t_2}/P_{t_0}	= inlet total pressure recovery
$\bar{T}$	= rms turbulence
T_{t_0}	= freestream total temperature
α	= angle of attack
β	= angle of sideslip
ρ	= first ramp position
$\Delta 3$	= third ramp position

Introduction

THE requirements for the inlet design on virtually any aircraft are to provide flow of sufficient uniformity to the engine to preclude stalls, and to operate with high total pressure recovery and low spillage drag to enhance aircraft performance. This design task clearly becomes more difficult for an air superiority aircraft such as the F-15, whose capabilities include high maneuverability and speed, together with good subsonic range. This factor, coupled with the then recent inlet-engine compatibility problems on the F-111A, resulted in much effort being expended in the development of the F-15 inlet.

The F-15 aircraft is built by the McDonnell-Douglas Corporation. The twin engine, single place airplane has a high thrust-to-weight ratio (greater than 1.0) and low wing loading to enhance its maneuverability. The aircraft has a fixed wing with no leading edge devices, twin vertical tails, and closely spaced twin convergent-divergent nozzles. The inlets are located adjacent to the side of the fuselage, forward of the wing. The aircraft is powered by two F-100 afterburning turbofan engines, which were developed by Pratt & Whitney. First flight of the aircraft occurred on schedule in July 1972.

Inlet/Control System Description

The inlet, shown schematically in Fig. 1, is two dimensional with horizontal ramps (three compression ramps and a diffuser ramp). This concept was selected to provide a uniform inlet flowfield at high angles of attack at supersonic speeds. It is an external compression inlet and at higher speeds produces a system of three oblique and one normal shock ahead of the cowl. Boundary-layer bleed is provided through porous regions on the second and third ramps, and through the throat slot. Additionally, bleed is removed on both sideplates in the vicinity of the normal shock. Typical distribution of the bleed is about 15% on the ramps, 70% through the throat slot, and 15% through the sideplates. The bleed from each of the ramps and the slot is exhausted through different sets of fixed louvers on top of the inlet. A bypass system is included in the inlet design to enhance inlet-engine matching at supersonic speeds where engine airflow decreases (such as at high altitude) and to fine tune the match point location to optimize performance. Bypass flow is removed from the inlet through the throat slot. The inlet has a moderately blunt lip, inclined at about 12° angle from the horizontal. The inlet sideplates are quite full (i.e., large sideplate area) because of the benefit of this shape on supersonic pressure recovery. Finally, the subsonic diffuser is relatively long, being about six engine diameters in length. The placement of the engine relative to the inlet precludes severe bends in the diffuser.

Figure 2 depicts the inlet variable geometry and the associated inlet control system parameters. The most unique feature of the inlet is its variable capture area, the advantages of which will be discussed later. Its variation is accomplished by rotating the entire forward ramp system as a unit about a point near the lower cowl lip. The included angle of the inlet leading edge is fixed so that changing the capture area also changes the first ramp deflection angle. The capture area is

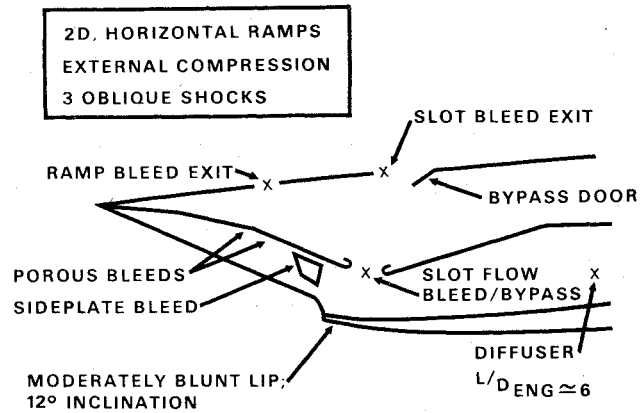

Fig. 1 Inlet description.

Presented as Paper 74-1061 at the AIAA/SAE 10th Propulsion Conference, San Diego, Calif., Oct. 21-23, 1974; submitted Oct. 29, 1974; revision received May 12, 1975.

Index categories: Airbreathing Propulsion, Subsonic and Supersonic; Aircraft Powerplant Design and Installation.

*Aerospace Engineer.

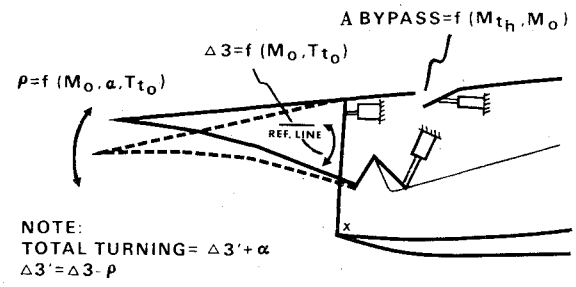

Fig. 2 Inlet control system.

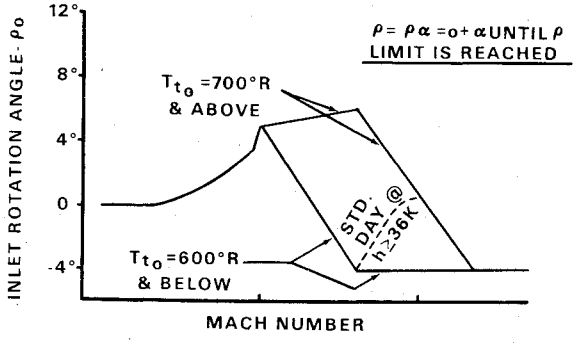

Fig. 3 First ramp schedule, $\alpha = 0°$.

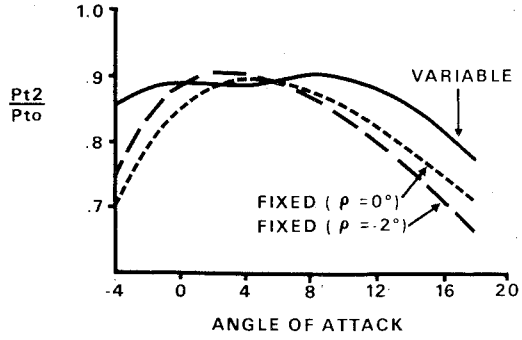

Fig. 4 Fixed vs variable capture recovery; $M = 2.2$.

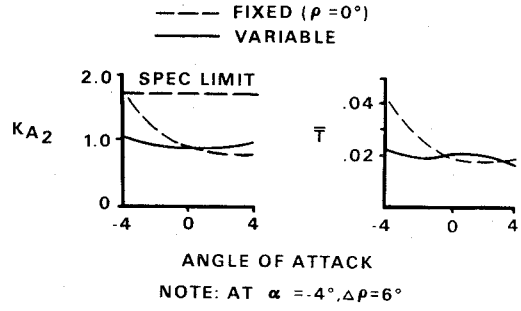

Fig. 5 Fixed vs variable capture distortion; $M = 2.2$.

varied as a function of Mach number, angle of attack, and freestream total temprature. The third ramp is linked to the diffuser ramp, and is scheduled as a function of Mach number, and freestream total temperature. The second ramp is slaved to the third ramp. In order to enhance matching at hot-day or low-altitude conditions, where engine corrected airflow diminishes, a temperature bias increases the third ramp angle. For purposes of control system mechanization, the third ramp parameter, Δ3, is defined relative to an inlet reference line, which moves with the capture area. Thus, the third ramp is really scheduled relative to the first ramp, and the absolute deflection angles are related to the freestream airflow by the equations shown in Fig. 2. The bypass system is aerodynamically closed loop, such that the door is positioned to provide a desired throat Mach number. This desired throat Mach number is in turn scheduled as a function of freestream Mach number.

Figure 3 shows the first ramp, and hence capture area, schedule for 0° angle of attack vs Mach number. The total available rotation range is 15°, and the sign convention used is inlet full-up (maximum capture area) at −4° and full-down at +11°. As indicated in the figure, the rotation angle at any given angle of attack is simply the sum of the rotation angle at 0° angle of attack plus the angle of attack, within scheduled limits (not depicted). The variation in the schedule, which is smoothed out some by the limits, results from different governing factors in different speed regimes. At very low speeds, this schedule has been motivated by the effect of the inlet on aircraft longitudinal stability. At higher subsonic and low and moderate supersonic speeds, the schedule and limits have been selected primarily to optimize drag. At higher supersonic speeds, the main factors have been pressure recovery and compatibility considerations, including distortion and stable range. The transonic temperature bias reduces the capture area at altitudes below 36,000 ft to relieve structural loads.

The third ramp control is quite conventional in that it is fixed relative to the first ramp up to low supersonic speeds, and then the deflection angle is increased with increasing Mach number. The hot-day trimming function is implemented by incorporating two schedules for supersonic speeds, one as a function of Mach number and the other as a function of temperature. On standard days above 36,000 ft, both schedules yield the same value, whereas at other conditions the larger value is selected. As noted previously, the bypass door is controlled to provide a desired throat Mach number (i.e., throat pressure ratio). The bypass is closed at subsonic Mach numbers.

Configuration Development

Inlet Integration

Initial pressure recovery and distortion data indicated that the fuselage forebody caused an adverse effect on inlet performance at higher supersonic speeds, and led to fuselage flowfield studies. Subsequent testing indicated that low energy air was being ingested by the inlet at conditions of leeward sideslip, and at high angles of attack without sideslip. The problem was alleviated by modifying the cross-sectional shape of the fuselage forebody. Specific changes consisted of rounding the bottom, increasing the lower corner radius, and raising the maximum fuselage width to a level above the inlet. Elevating the nose reduced downwash and downwash gradients across the inlet area at low angles of attack with leeward sideslip. This finding was beneficial because downwash decreases the effectiveness of the first inlet compression ramp. This overall approach to fuselage/inlet integration is considered likely to result in a lower drag and/or lighter weight aircraft as compared with simply moving the inlet far enough outboard to be out of any adverse forebody flowfield effects.

Initial wind-tunnel testing presumed, as it typically does, that the inlet variable geometry would be in the exact positions that the control schedules define. In reality the aircraft pitot-static tubes and angle of attack sensors, which provide the inputs to the inlet control system, are within the influence of the aircraft fuselage. Consequently, local flowfield effects at these sensors (i.e., local value of the variable different than the freestream value) were defined. Correction curves are mechanized in the inlet control system to remove these systematic effects at 0° sideslip. However, in order to minimize control system complexity, the variation of the local flowfield during sideslip is not corrected for, and the inlet variable geometry deviates from its nominal (0°sideslip) position. To address this factor, the variations due to sideslip

were defined, and the corresponding deviations in ramp positions (relative to their scheduled values at 0° sideslip) then were computed. These deviations then were set on the inlet model during subsequent wind-tunnel testing with sideslip conditions, thereby properly accounting for real-world control system behavior.

The most important interface in the inlet development was that with the engine, and this interface received the most attention. The methodology for evaluating engine face total pressure distortion has been geared closely to the Pratt & Whitney methodology for assessing engine tolerance to distortion. This approach involves evaluation of the engine face contour plots as described by high response instrumentation. This instrumentation responds to all total pressure oscillations up to the maximum frequency of interest to the engine, adjusted appropriately for model scale. In this case, where a 1/6th scale model was used, data were processed through an electronic filter, having the characteristic of attenuating the pressure magnitude by 30% at 1000 cps. This filter characteristic was determined in prior experimental testing to best correlate engine stalls due to high-frequency total pressure fluctuations. The evaluation of the contour plots involves calculation of numerical indices defined by empirical equations, which account for the level and spatial distribution of low and high total pressure regions. At any given operating condition, a corresponding value of the index defines the engine distortion limit. In addition to the indices, rms turbulence was computed for all test points. In order to assist in data handling and analysis, McDonnell developed an analog computer to calculate these values on line during the test.

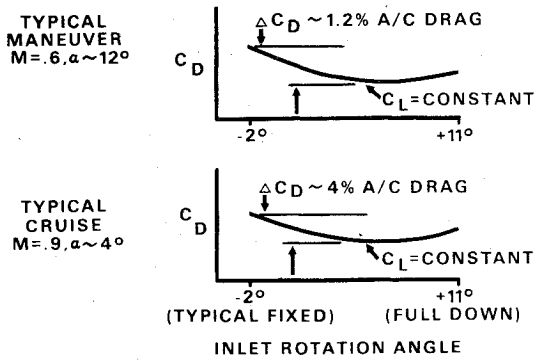

Fig. 6 Trimmed aircraft drag vs inlet position.

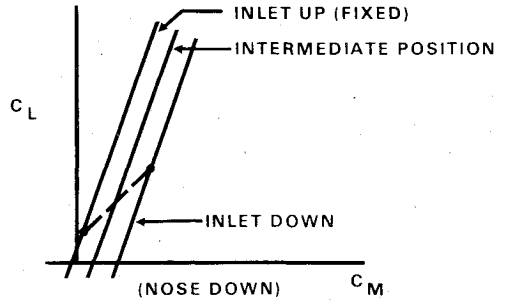

Fig. 7 Pitching moment effects, tail off; $M=0.9$.

Inlet Design

The wind-tunnel test programs, which were conducted to optimize inlet behavior, examined alternate configurations for many of the individual elements that comprise the overall inlet design. This paper will discuss fixed vs variable capture area, the inlet boundary-layer bleed system, the shape of the third compression ramp, bluntness of the lower cowl lip, and the shape of the inlet sideplates.

Fixed vs Variable Capture Area

Both fixed and variable capture area inlets were carried as competitive designs well into the F-15 development program. The initial motivation for the variable capture area inlet was to maintain a well-behaved shock structure (e.g., three oblique and a normal shock of approximately equal strengths) over a wider range of angle of attack at high supersonic speeds. The benefits of such shock system behavior, as it affects inlet total pressure recovery and instantaneous total pressure distortion, are depicted in Figs. 4 and 5, respectively. Whereas the fixed capture recovery clearly peaks out in the region of 1° to 5° angle of attack, the variable capture recovery is maintained relatively constant for angles of attack of −2° to 12°. The reduced distortion and turbulence shown in Fig. 5 at negative angles of attack for the variable capture result from the increased first ramp compression produced by upward rotaion (2° more for the data presented than in the control schedule finally selected).

As part of the fixed vs variable capture area investigation, wind-tunnel testing examined the effects of different inlet rotation angles on aircraft drag. At subsonic conditions, the inlet rotation angle does not appreciably influence recovery or distortion. Therefore, flexibility existed for evaluating potential benefits to aircraft performance. Typical observations from the wind-tunnel tests were that, at a given angle of attack, inlet rotation angle influenced both drag and pitching moment. Since the latter influenced aircraft trim drag, it became necessary to evaluate trimmed aircraft drag vs inlet position. Figure 6 shows such data at typical subsonic maneuver and cruise conditions. It can be seen that use of the variable capture area (inlet rotation angles of other than −2°) offered the potential for drag reduction of the order of 1 to 4%, as compared to the fixed capture design. The effects on aircraft pitching moment are illustrated schematically in Fig. 7. At a given lift coefficient, reducing the inlet capture area increases the nose down pitching moment. Consequently, with the variable capture area, as aircraft angle of attack increases and the inlet rotates down, the aircraft is inherently more stable (as depicted by the dotted line in Fig. 7) than with the inlet fixed. The final inlet control schedules, which were described earlier, were selected to best take advantage of these characteristics. The final inlet rotation schedule also relieves loads in the inlet backup structure due to two factors. First, rotating the inlet down at high angles of attack lowers its incidence angle relative to the airstream. Secondly, a similar result occurs at transonic speeds below 36,000 ft because of the temperature bias in the inlet rotation schedule, cited earlier.

Bleed System

The inlet bleed system optimization program investigated the effects on inlet performance of varying the amount of bleed flow removed from the second and third compression ramps, the sideplates, and the throat slot. A parametric test program was conducted during which the bleed sources were systematically varied to determine the effects on recovery, instantaneous distortion, and subcritical stable range. Each source was varied individually from no flow to approximately the following percentages of maximum captured flow at Mach 2.2:1% from the second ramp, 1.5% from the third ramp, 1.5% from the two sideplates combined, and 5% through the throat slot. Test results indicated considerable interaction between the various bleed sources. That is, the effectiveness of one source was frequently dependent on the flow rates through the other sources. The benefit of bleed flow off the second and third ramps and sideplates was maximized at intermediate levels, i.e., between no flow and the largest flow rates tested. Table 1 summarizes the trends observed. The adverse effect on stable range of larger ramp bleed rates is likely because of reduced boundary-layer bridging between the ramps (which decreases the third shock angle) and/or increasing the effective inlet face area (which moves the normal

Table 1 Bleed source summary

Source	Observations
Sideplate	1. Some improves recovery 2. Too much can increase distortion
2nd ramp	1. Results depend on 3rd ramp bleed level 2. Some improves recovery and distortion small amount (when have small 3rd ramp bleed) 3. Too much reduces stable range and slightly increases distortion
3rd ramp	1. Results depend on 2nd ramp bleed level 2. Small amount can slightly increase stable range, but too much reduces
Throat slot	1. Very beneficial to recovery and distortion when low ramp bleed rates 2. Never reduces recovery or distortion

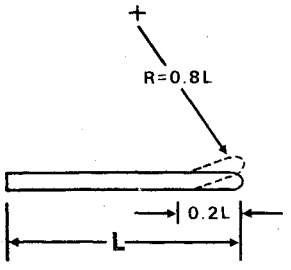

Fig. 8 Curved third ramp.

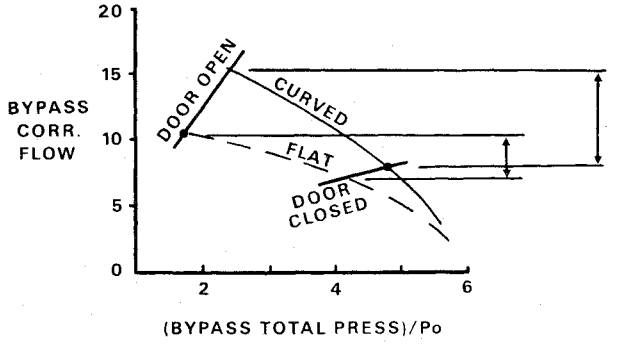

Fig. 9 Curved third ramp effect on bypass operation; $M=2.2$, $\alpha=0°$.

shock forward). Either effect brings the oblique-normal intersection closer to the third ramp, thereby precipitating buzz at a higher mass flow. It was concluded that the best configuration was to bleed small amounts from the second and third ramps and sideplates, and to use the throat slot as the main bleed source. Typical bleed flow rates for this configuration (as percent of maximum captured flow) at Mach 2.2 are: 0.5% for the second and third ramp and 3.5% for the throat slot.

Throat Slot Geometry

In addition to the throat slot being an effective bleed removal source, it also was selected as the location for removing bypass flow. This dual role of the slot allowed a reduction in aircraft weight in contrast to a separate bypass system further aft in the duct. Having established that a throat slot would be included, various modifications to the third and diffuser ramps were made in the vicinity of the slot to determine their effects on inlet and bypass system performance. The main configuration change that resulted was to curve the third ramp forward of the slot. This change, shown schematically in Fig. 8, increased the captured flow resulting in an inlet-engine match at a slightly higher recovery. Additionally it increased the bypass system total pressure and

DISTANCE AFT OF LEADING EDGE	THICKNESS OF SHARP	THICKNESS OF BLUNT
0.5"	0.62"	0.88"
.1"	0.88"	1.16"
.2"	1.25"	1.60"
.3"	1.63"	1.90"

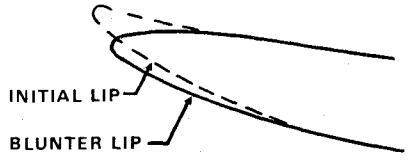

Fig. 10 Alternate cowl lip shapes.

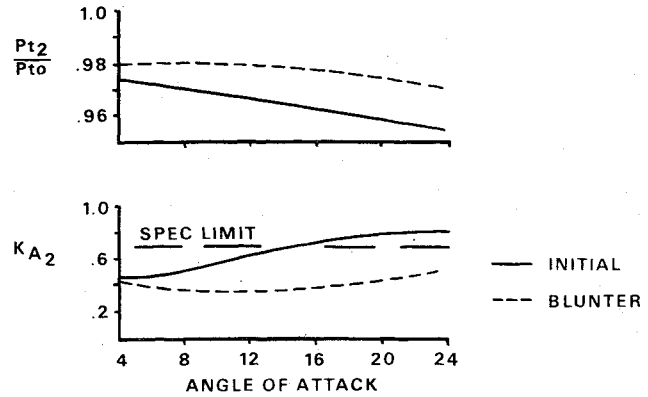

Fig. 11 Lip improvement; $M=0.9$.

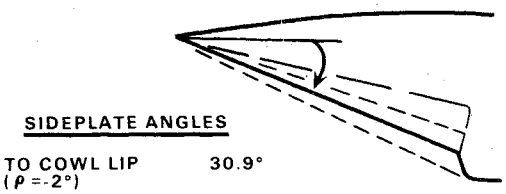

SIDEPLATE ANGLES	
TO COWL LIP ($\rho=-2°$)	30.9°
FULL SIDEPLATE	26.7°
PARTIAL	22.1°
MAX CUTBACK	15.7°

Fig. 12 Sideplate geometry.

flow, because of smoother turning of the flow into the slot. This latter effect is shown in Fig. 9.

Lower Cowl Lip Shape

The idea of blunting the lower cowl lip to delay lip separation at high angles of attack at subsonic speeds, thereby improving recovery and distortion, is well known. This factor was explored in F-15 wind-tunnel testing. Figure 10 illustrates the two lip shapes tested. The results are shown in Fig. 11 to give an indication of the magnitude of changes observed in recovery and distortion. Testing at Mach 1.6 and 2.2 revealed no drag penalty due to this change.

Sideplate Shape

The shape of the inlet sideplates was investigated to determine the effect on inlet behavior. The alternate shapes tested are shown in Fig. 12. Figure 13 shows comparative data at 0° angle of attack and sideslip. The cutback design has similar recovery, but offers small improvements in distortion and subcritical stable range. Note that the cutback sideplates reduce the maximum captured flow (likely due to increased sidespill), therby effectively reducing inlet size. Figure 14 depicts comparative behavior at a severe attitude. It can be seen that increased cutback appreciably improves recovery and distortion. The configuration selected for use on the aircraft was the "full sideplate" shape, but with boundary-layer

bleed removal incorporated on the sideplate. This resultant configuration was chosen because it improved 0° sideslip recovery by 1.2% above that shown in Fig. 13.

Summary Inlet Data

The F-15 development program included a full-scale inlet-engine wind-tunnel test. This testing was performed at subsonic and supersonic speeds and covered an angle of attack range of −4° to 11°. A partial forward fuselage was included to duplicate the Mach number and flow angularity ahead of the inlet which exists on the actual aircraft. As an outgrowth of this test program, data were obtained which, when combined with prior model and subsequent flight test results, afforded an opportunity to compare inlet performance data between the three sources.

Model vs Full-Scale Wind-Tunnel Data

A comparison of inlet total pressure recovery at Mach 0.6 and 0.9, 4° and 11° angle of attack, showed the 1/6th model and the full-scale inlet data to be almost identical at part power airflow. At maximum airflow (intermediate power and augmented engine operation) the recoveries were within 1%, with the full-scale values being higher. At Mach 2.2, the model and full-scale data are within about 1% at low angles of attack, but at higher angles of attack the full-scale recovery is almost 2% higher. This trend was observed both with a set of ramp angles which were devised to operate with early PFRT engines, and for production ramp schedules which had reduced supersonic turning of the flow.

Figure 15 compares peak instantaneous distortion at Mach 0.6 and 0.9 in terms of the Pratt & Whitney distortion index, and indicates quite good agreement between the model and full-scale data. The engine specification limits are identified to give an indication of the relative magnitudes of the data points plotted. Figure 16 reveals a similar comparison at Mach 2.2. Analogous to the recovery data, agreement is good at low angles of attack. At 11° angle of attack, where the disagreement is larger, the full-scale behavior is superior to the model. Qualitatively, at most conditions, the steady-state and peak instantaneous distortion patterns have similar characteristics in comparing model and full-scale data. However, at subsonic conditions the model data had a slightly stronger radial pressure gradient.

Comparison with Flight Test Data

Consistent with the close agreement in subsonic pressure recovery between model and full-scale wind-tunnel data, subsonic recovery observed in flight agreed well with these other two data sources. Before comparing supersonic flight test data with wind-tunnel results (both recovery and distortion), it is important to point out some of the complications that make precise supersonic comparisons difficult. First, model and full-scale inlet wind-tunnel tests were run in almost all cases with the bypass full open or closed. In flight, because of either the use of early version engines, engine to engine variations, or nonstandard temperatures, the bypass can be operating at a partially open position. The amount of bypass flow influences recovery and/or distortion at higher supersonic speeds. Secondly, in order to expedite flight test data acquisition and to assure proper inlet operation in flights to high speed, data at these conditions typically are acquired with the inlet under control of the automatic control system. (The first two test aircraft also have manual control provisions to permit control schedule optimization testing.) Consequently, as a result of the temperature bias in the first and third ramp control schedules described earlier, flight at nonstandard temperatures causes deviations in ramp angles from the values set in the wind tunnel. At this time the computerized data reduction and subsequent analysis effort is sorting out these effects, since the final inlet schedule optimization program now is completed.

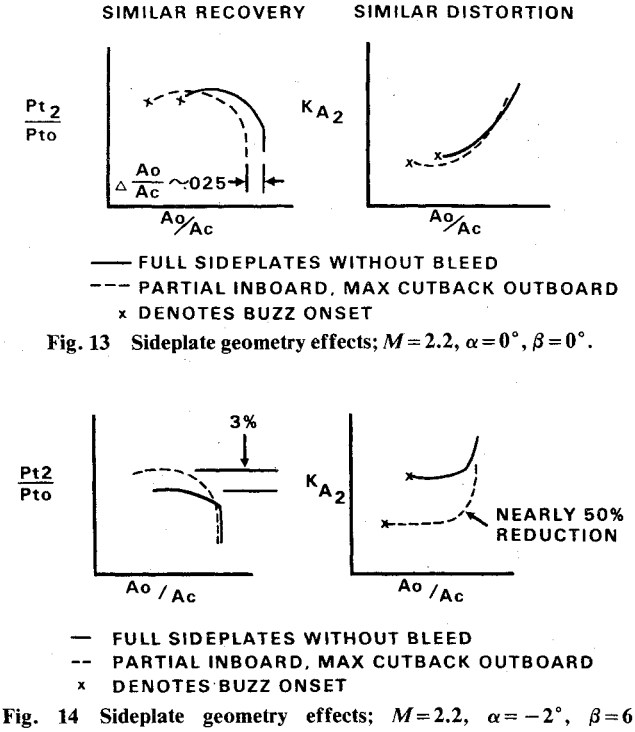

Fig. 13 Sideplate geometry effects; $M=2.2$, $\alpha=0°$, $\beta=0°$.

Fig. 14 Sideplate geometry effects; $M=2.2$, $\alpha=-2°$, $\beta=6°$ leeward.

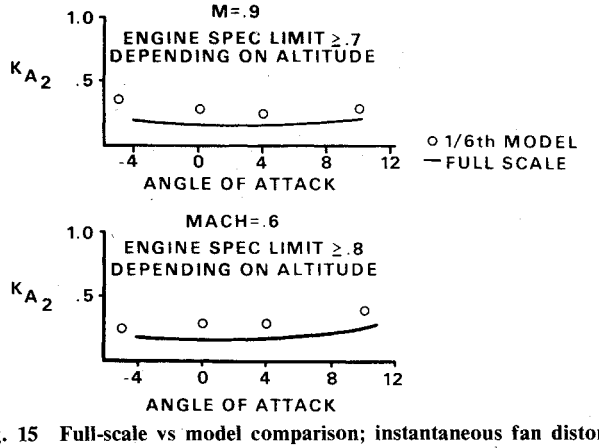

Fig. 15 Full-scale vs model comparison; instantaneous fan distortion.

Recognizing these factors, the supersonic recoveries measured in flight agree within about 1% of the predictions based on wind-tunnel results. Recalling from the last section that the full-scale wind-tunnel recovery exceeded the model values at Mach 2.2, flight results to date fall within the band of wind-tunnel data.

With respect to instantaneous inlet distortion, the full-scale wind-tunnel data agree well with the flight test data. Figure 17 shows such a comparison at Mach 0.6 and 1.8. The engine specification limits are again shown to give an indication of the relative magnitude of the data presented. The engine airflows are sufficiently close to give a meaningful comparison.

A comparison of 1/6th scale model with flight test distortion data is made in Fig. 18. The right curve dipicts a subsonic comparison over a large angle of attack range at 0° sideslip. All data shown are at the same engine airflow. It can be seen that the distortion measured in flight is lower than the model data when measured with the expanded scale data acquisition system (6.5 psia range). The scatter between the two sets of symbols shown is at least in part caused by the differences in resolution between the two ranges noted in the data recording system. This conclusion is based on the systematic differences and the fact that all data points between 4° and 16° angle of

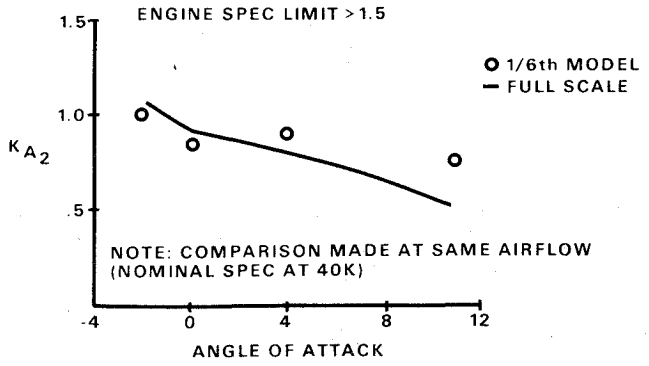

Fig. 16 Full-scale vs model comparison; instantaneous fan distortion; $M = 2.2$.

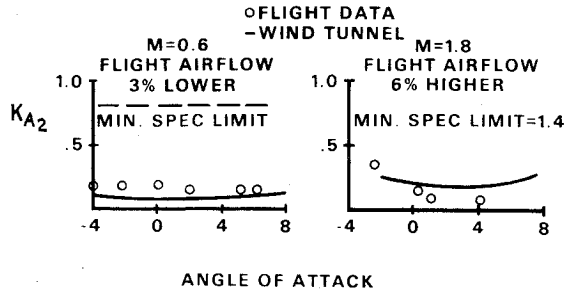

Fig. 17 Full-scale wind tunnel vs flight comparison; instantaneous fan distortion.

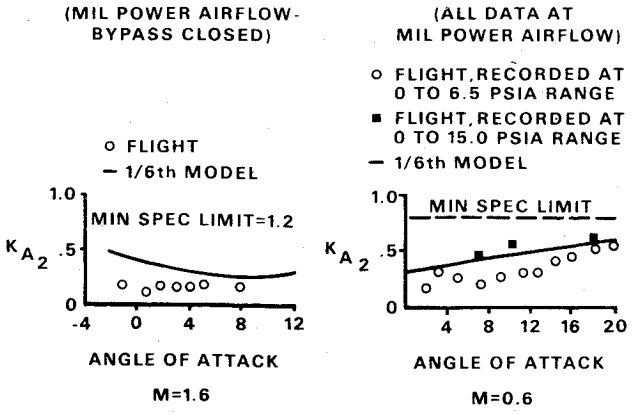

Fig. 18 Model vs flight comparison; instantaneous fan distortion.

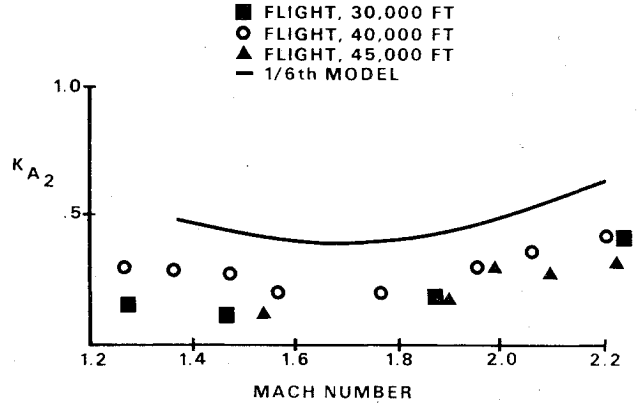

Fig. 19 Model vs flight comparison; instantaneous fan distortion; supersonic lg.

attack were obtained at 30,000 ft, except for the high data point at 10°. This latter point was obtained at 45,000 ft, where the resolution of pressure is more difficult. The other curve in the figure shows a similar comparison between model and flight data at Mach 1.6. Again, the flight distortion levels are lower.

Since the in-flight distortion being lower than the model is favorable from an airplane development standpoint, and no inlet-engine compatibility problems have been uncovered in flight, an exhaustive investigation has not been performed to explain these results. However, distortion indices have been computed which exclude radial distortion. A comparison between model and flight data for that index has been made over the Mach range of 0.6 to 1.6, and closer agreement is obtained. This result suggests that the model experienced some difference in radial distortion as compared to the aircraft. This conclusion is not inconsistent with the observation made earlier that the model data had a stronger radial pressure gradient than the full-scale wind-tunnel inlet at subsonic Mach numbers. Further, the Mach 0.6 data in Fig. 18 show closer agreement between model and full scale at the highest angles of attack, where circumferential distortion is contributing more to the total distortion.

Figure 19 presents a comparison vs Mach number for 1 g supersonic flight. The model data were selected at airflows similar to those experienced in flight. Again, the flight test distortion is always lower than the model. The apparent systematic difference below Mach 1.6 between data acquired at 30,000 ft and those obtained at higher altitude has not been fully explained. It is important to recognize, however, that differences in K_{A2} of 0.1 are within the accuracy of measurement and calculation. Concerning the disagreement between the flight and model data, a possible explanation for results at Mach 1.6 and below was given previously. The distortion level differences at higher Mach numbers have not been identified fully, although a couple of factors could be contributing. The difference between model and full-scale radial distortion is not considered to be contributing significantly to the K_{A2} differences, since at these higher Mach numbers the inlet patterns from both sources are predominantly circumferential in character. Deviations in ramp positions due to nonstandard temperatures in flight may well be causing part of the disagreement. (Model data are presented for standard day ramp schedules.) Recalling the schedules for the first and third ramps at higher Mach numbers, the first ramp will not respond to temperatures higher than standard day, but will provide increased compression on cold days. Conversely, the third ramp (and second) will not respond to temperatures below standard day values, but will provide increased compression on hot days. Thus, for any in-flight deviations in temperature from standard day values at these speeds, the inlet schedules will cause increased compression through the oblique shock system. This suggests systematically weaker terminal shocks in flight as opposed to the model data. Also, at Mach 1.8, the model data were obtained with the flat third ramp and the bypass closed, whereas the flight test data were acquired with the curved third ramp and the bypass open. As a final note, the Mach 2.2 model distortion levels shown in Figs. 16 and 19 are different because of differences in bypass door position, and to a lesser degree because of small differences in engine airflow.

Conclusions

The F-15 inlet development program has been successful, to a large degree, because of the comprehensive wind-tunnel program, which addressed both the inlet integration and design early in the overall aircraft development effort. The program was enhanced further by very close coordination throughout between the airframe and engine manufacturers. Significantly, a consistent methodology for evaluating inlet-engine compatibility was employed as work progressed from subscale model wind-tunnel testing to aircraft flight testing.